Polarons in electron-populated quantum dots revealed by resonant Raman scattering

B. Aslan,* H. C. Liu,† M. Korkusinski, P. Hawrylak, and D. J. Lockwood
Institute for Microstructural Sciences, National Research Council, Ottawa, Ontario K1A 0R6, Canada
(Received 24 May 2006; published 26 June 2006)

We report on the direct observation of polarons in InAs/GaAs self-assembled quantum dots (QD) populated by few electrons. The polarons are strongly coupled modes of QD phonons and electron intersublevel transitions. The degree of coupling is varied in a systematic way with a set of samples having electron intersublevel spacing changing from larger to smaller than the longitudinal-optical-phonon energy. The signature of polarons is evidenced clearly by the observation of a large (12–20 meV) anticrossing for both InAs and GaAs-like QD phonons using resonant Raman spectroscopy.

DOI: 10.1103/PhysRevB.73.233311 PACS number(s): 78.67.Hc, 73.21.La, 78.30.Fs

The general problem of the pairing of strongly interacting elementary excitations producing new quasiparticles arises in many areas of solid state physics; for example, there are polarons involving electron motion and a lattice vibration, polaritons involving electronic polarization and a photon, biexcitons in semiconductors, and Cooper pairs in superconductors. Recently there has been significant interest in polaron formation in semiconductor quantum dots (QDs), which can be thought of as artificially engineered atoms.[1–5] This is motivated by the need to understand the nature of the carrier relaxation processes and their role in quantum dot based devices such as infrared photodetectors and lasers as well as in the application of quantum dots in quantum information processing. In QDs, phonon-assisted energy relaxation is expected to be slow at energies different from the longitudinal optical (LO) phonon energy because of the discrete nature of the electronic energy levels.[6] This inefficient energy relaxation process is known as the "phonon-bottleneck."[7] However, relatively fast relaxation times have been observed in QDs, and alternative mechanisms, such as multiphonon-assisted (acoustic and/or optical)[8] and Auger-type relaxation processes (for high carrier densities),[9] have been proposed. Recently, it was shown that the electrons and phonons should be strongly coupled in QDs leading to the formation of polarons.[1] The first indications of strongly coupled electron-phonon modes in InGaAs QDs[2,3] were attained by applying a high magnetic field, which brought the electronic transition energy into resonance with either an AlAs-like interface phonon[2] or multiple bulklike GaAs phonons,[3] leading to a small (2–4 meV) anticrossing in far-infrared magnetotransmission spectra. Very recently, indirect evidence of polaron formation was observed in photoluminescence (PL) spectra by using coupled quantum dots separated by a varying barrier width[4] and by using a magnetic field[5] to tune the electronic energy level.

In this article we report on the direct observation of polarons involving single intrinsic QD phonons in a set of *n*-doped InAs self-assembled QD samples whose intersublevel energy spacings are tuned across the LO-phonon energy by a postgrowth annealing process. The samples where the quantum dot energy level spacing matches the LO-phonon energy are in the strong coupling regime. The polaron modes are detected by resonant Raman scattering,[10,11] where the laser excitation energy is in resonance with the QD interband *s*-shell. We stress that this technique is absolutely essential for enhancing the polaron Raman signal from the QDs.

The quantum dot samples used in this study were grown by molecular beam epitaxy on (100) GaAs substrates (see Ref. 12 for additional details). Between the top and bottom doped GaAs layers, the samples consist of 50 layers of self-assembled InAs QDs separated by 30-nm GaAs barriers modulation doped with Si to populate the QDs with electrons. From the quantum dot density and the level of doping, it is estimated that the average population per QD was ~7 electrons for the sample whose results are presented here. Other samples with different electron numbers per dot were also investigated and the results were qualitatively the same. To tune the QD level spacings, small pieces from the same part of the uniform wafer were treated by rapid thermal annealing at different temperatures for 30 s under N_2 ambient (samples *j* and *k* were annealed with a GaAs capping piece on top of them). For PL and Raman measurements, the samples were maintained at 14 K on the cold finger in a He flow cryostat. For PL experiments, a 532-nm frequency-doubled $Nd:YVO_4$ laser was used as the excitation source and the spectrum was analyzed by a Fourier transform infrared spectrometer (FTIR) with an InGaAs detector. The Stokes Raman measurements were carried out by using a double-grating-subtractive monochromator as a filter in conjunction with the FTIR; a Ti:sapphire laser, continuously tunable in the spectral range from 0.9 to 1.1 μm, was used as the excitation source. The Raman experiments were performed in a near-back-scattering geometry with a ~45° incident angle.

The tuning of the quantum dot level spacing is depicted in Fig. 1(a), which displays low temperature emission spectra of highly excited as-grown and annealed samples. The structures labeled "*s*, *p*, *d*" correspond to emission from populated shells of quantum dot energy levels. As the annealing temperature is increased, the spacing and broadening of emission from various shells are decreased simultaneously with a pronounced blueshift of the emission energy.[13] These PL spectra show that our QDs are quite uniform in size and that the annealing produces a systematic change. Fig. 1(b) shows the level spacing extracted from PL spectra of Fig. 1(a): the spacings of *s*- and *p*-shells and *p*- and *d*-shells decrease with annealing temperature, and eventually become lower than the bulk GaAs LO phonon energy of 37 meV. It

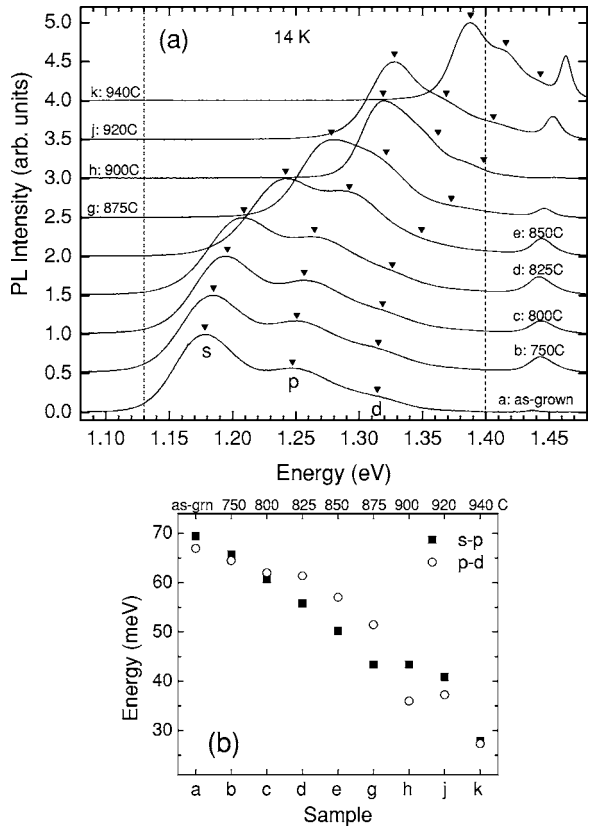

FIG. 1. (a) Low temperature PL spectra for as-grown and annealed samples. Temperatures at which the samples were annealed for 30 s are marked beside each plot. The structures labeled "*s*, *p*, *d*" and marked for each curve correspond to emission from populated shells of quantum dot energy levels. Vertical dashed lines show the tuning limits of the Ti:sapphire laser used for the Raman scattering experiments. (b) Energy level spacings extracted from the PL.

should be noted that the transitions from the *p*- and especially *d*-shells are seen less clearly in Fig. 1(a) for some of the samples annealed at higher temperatures; however, the level spacings were readily extracted by investigating the excitation power dependence of the PL curves. The energies used for the shell level extraction were also marked by points on each curve in Fig. 1(a) as a guide for the eye. The exact conduction band intersublevel spacing corresponds to about 70% of the shell spacing extracted from PL.[14] The origin of the decrease in the level spacing is the interdiffusion of the dot and the barrier materials on annealing. To show the annealing effect, we calculated electron energy levels in the effective mass approximation by taking the compositional profile and the strain distribution into account (results are not presented here). These calculations do not match experiment quantitatively due to the simplicity of the model and the lack of a detailed knowledge of the actual QD shape. Yet the theory in its present form shows qualitative agreement with experiment; it shows that by changing the atomic diffusion length with increasing annealing temperature, the spacing of energy levels can be tuned through the optical phonon energies.

We now turn to the Raman scattering results. A typical spectrum of the as-grown sample measured for low excitation energy (1.168 eV, slightly below the ground state transition energy) is shown in Fig. 2(a). The distinct sharp features observed at 295, 282, 271, and 239 cm^{-1} are due to the GaAs layer LO, GaAs-like QD LO, GaAs layer transverse optical (TO) and InAs WL LO phonons, respectively. Another weaker feature appearing at 259 cm^{-1} is attributed to the LO phonons of the InAs QDs. It has been theoretically predicted that the average strain-induced shift of the LO phonon energy in the InAs QD is 2.2 meV;[15] using the bulk LO phonon frequency of 239 cm^{-1}, it gives 257 cm^{-1} for this mode—in good agreement with our experimental value. The broad feature appearing at higher frequency ($\sim$460 cm^{-1} =57 meV) originates from intersublevel transitions. When the QDs are excited with lower energies ($<$1.160 eV), features due to the GaAs-like phonon and intersublevel transition disappear (not shown). Fig. 2(b) shows the spectrum for an excitation energy of 1.198 eV, which is slightly above the ground state transition energy. The GaAs LO and TO phonons are not distinguishable anymore because of the very intense GaAs-like phonon signal, which is enhanced together with the signal from the electronic transition for all such higher excitation energies. Note that the scales of the graphs reflect the relative increase in the intensity, demonstrating the power of resonant enhancement. Sharp cuts at both edges of the spectra are due to the subtractive monochromator light-rejection window and the low frequency feature is the tail of the strong laser signal.

Raman spectra for as-grown and annealed samples, taken under similar conditions to the one in Fig. 2(b), are presented in Fig. 3(a). The signal originating from the intersublevel transition at the high energy part of the spectrum clearly

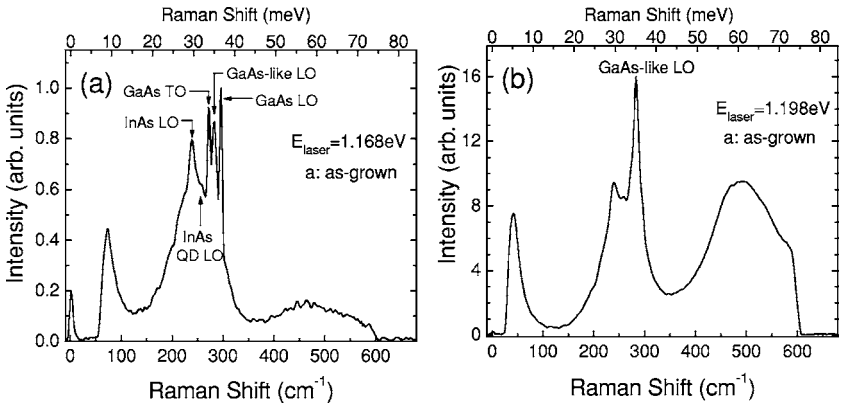

FIG. 2. Low temperature Raman spectrum of the as-grown sample measured for excitation energies (a) slightly below and (b) slightly above the ground state transition energy.

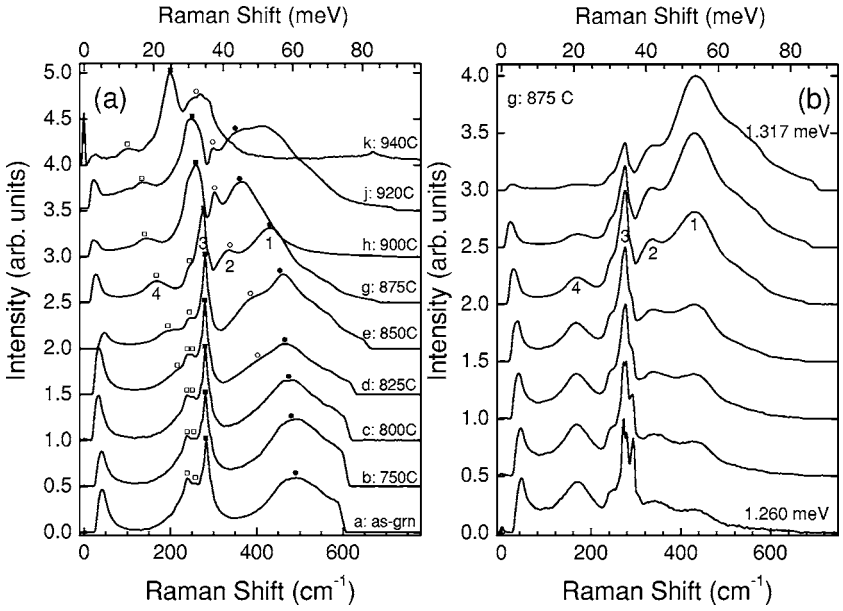

FIG. 3. (a) Low temperature Raman spectra taken under resonance conditions for as-grown and annealed samples. Numbered peaks are the subject of this study. (b) Evolution of the Raman spectra with excitation energy for sample g, annealed at 875 °C.

approaches the phonon energy region as the annealing temperature increases. Two new features appear on either side of the phonon region for samples annealed above 825 °C. The evolution of the aforementioned peaks [denoted as peaks 1 to 4 in one of the curves in Fig. 3(a)] with excitation energy for sample *g*, annealed at 875 °C, is presented in Fig. 3(b). The relative intensity ratios of the peaks are changing with excitation energy. Note that each curve is normalized with respect to its maximum point. The signal strength actually increases significantly for higher excitation energies as the resonant condition is approached; for example, there is more than two orders of magnitude difference in scale between the bottom and top curves in Fig. 3(b). The wiggles appearing above 60 meV for the upper curves are attributed to second-order phonon combinations such as 2TO, TO+LO, and 2LO. Further increasing the excitation energy detunes the resonance condition and causes a strong PL signal that obscures the Raman signal. For a fixed excitation energy far away from strong coupling, similar Raman scattering by QD phonons and intersublevel transitions has been observed previously.[16,17]

In order to see how the Raman peaks evolve with annealing temperature, the positions of each peak [marked in Fig. 3(a)] versus sample are plotted in Fig. 4(a). While peaks 1 and 2 approach from higher energy to the phonon energy region, peaks 3 and 4 branch off from the lower part. The horizontal lines show for comparison the bulk phonon energies: solid lines are for LO and dashed lines are for TO phonons for both bulk GaAs (upper pair) and InAs (lower pair).

The phonon modes in QDs are more complicated than those in bulk semiconductors. Since the intersublevel dipoles are confined in the QD, we expect that the strongest coupling is with the InAs QD (confined or interface) phonon modes. Moreover, though expected to be weaker than the InAs QD phonon, there should be a GaAs-like mode due to the alloying effect (i.e., the dot is not pure InAs but rather InGaAs with a low Ga fraction, especially for the annealed samples). The GaAs bulk or other interface phonons have much weaker coupling to the intersublevel transitions.[2,3] The behavior shown in Fig. 4(a) can be qualitatively accounted for by the interaction of QD phonons and intersublevel transitions leading to the formation of polarons. The LO phonon

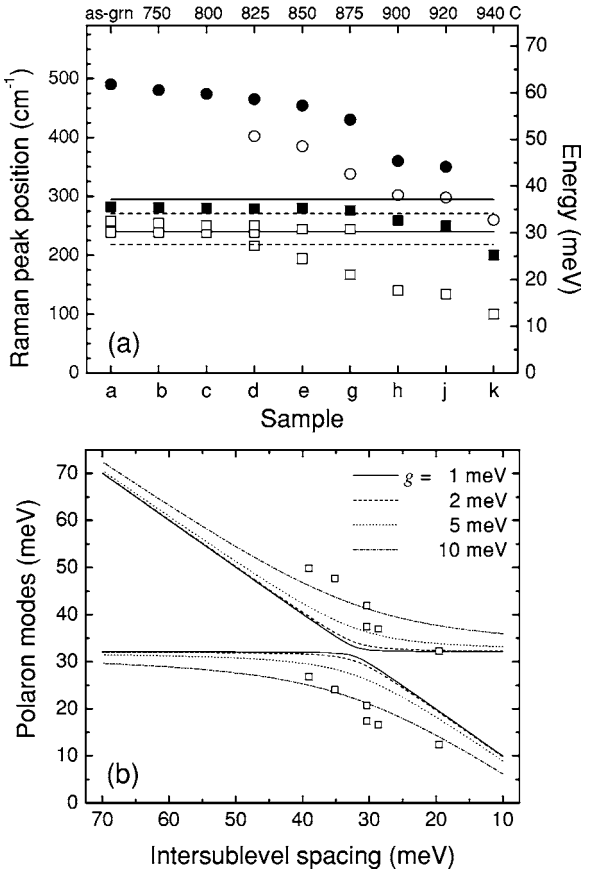

FIG. 4. (a) The positions of each peak marked in Fig. 3 vs sample designation. (b) Calculated polaron eigenmodes as a function of intersublevel spacing for $\hbar\omega_L$=32.1 meV and several values of the coupling constant *g*. Experimentally observed InAs QD polaron data points are shown with open squares.

with frequency ω_L sets up an electric field that varies slowly on the scale of the quantum dot. This electric field couples equally to all electrons in the quantum dot, hence it couples to the center-of-mass (CM) motion in the direction of the electric field of the phonon mode. The CM motion is only weakly coupled to the relative motion of electrons by the finite size of the quantum dot, as verified by an exact diagonalization study to be reported elsewhere. For quantum dots with nearly equal level spacing as shown in Fig. 1(b), the CM Hamiltonian is that of two harmonic oscillators. Only one of them couples to the longitudinal phonon. Hence the electron and phonon Hamiltonian can be written as a sum of coupled harmonic oscillators:

$$H = \hbar\omega_0(A^\dagger A + 1/2) + \hbar\omega_L(B^\dagger B + 1/2) + g(A^\dagger + A)(B + B^\dagger), \tag{1}$$

where coupling originates from displacement $R_x \sim (A^\dagger + A)$ of the CM and electric field $E \sim (B + B^\dagger)$ of the phonon mode, with g being the coupling constant, and $\hbar\omega_0$ and $\hbar\omega_L$ are the electronic level spacing and phonon energy. From Eq. (1) it is clear that the normal modes of the electron phonon system are coupled modes, i.e., polarons. For this model Hamiltonian, in which the higher-order coupling terms were neglected, polaron energies can be written as

$$E_\pm = (\hbar\omega_0 + \hbar\omega_L \pm \sqrt{\Delta^2 + 4g^2})/2, \tag{2}$$

with detuning parameter $\Delta = |\hbar\omega_0 - \hbar\omega_L|$. To assess the quality of this approximation, we have also performed an exact diagonalization calculation of the full Hamiltonian; the results are in very good agreement. Figure 4(b) shows the polaron energies obtained from Eq. (2) as a function of intersublevel spacing for $\hbar\omega_L = 32.1$ meV (the experimentally observed InAs QD LO phonon energy) and several values of the coupling constant. The open symbols in Fig. 4(a) display an anticrossing gap of $2g = 20$ meV, qualitatively matching the behavior shown by the $g = 10$ meV curve in Fig. 4(b). The experimentally observed InAs polaron data points given in Fig. 4(a) are also reproduced in Fig. 4(b); for this purpose, the intersublevel spacing was calculated by taking 70% of the *s*- and *p*-shell spacing extracted from the PL spectra [Fig. 1(b)]. Since the GaAs-like QD mode is due to an alloy of low Ga fraction, it is expected to be weaker than the InAs QD mode. The coupling is therefore expected to be weaker, leading to a smaller anticrossing gap. This is evidenced in Fig. 4(a) where the gap between open symbols is larger than that between solid symbols. An experimentally observed anticrossing gap of 12 meV for the GaAs-like QD mode is consistent with that predicted in Ref. 3.

In conclusion, we have directly observed the polaron excitation in InAs/GaAs self-assembled QDs using a systematic set of samples having electron intersublevel spacings changing from larger to smaller than the LO-phonon energy. In order to enhance the signal from the polaron—the coupled mode of QD phonons and electron intersublevel transitions—resonant Raman scattering has been used. The polaron picture is evidenced clearly by the observation of a large anticrossing for both InAs and GaAs-like QD phonons.

The authors thank P. Finnie for MBE growth, C. Y. Song for help in Raman experiments, and A. Delgado for discussions. This work was supported in part by a contract from U.S. AFRL/AFOSR via Anteon Corporation.

*Electronic mail: aslanb@nrc.ca
†Electronic mail: h.c.liu@nrc.ca

[1] T. Inoshita and H. Sakaki, Phys. Rev. B **56**, R4355 (1997).
[2] P. A. Knipp, T. L. Reinecke, A. Lorke, M. Fricke, and P. M. Petroff, Phys. Rev. B **56**, 1516 (1997).
[3] S. Hameau, Y. Guldner, O. Verzelen, R. Ferreira, G. Bastard, J. Zeman, A. Lemaitre, and J. M. Gérard, Phys. Rev. Lett. **83**, 4152 (1999).
[4] G. Ortner, R. Oulton, H. Kurtze, M. Schwab, D. R. Yakovlev, M. Bayer, S. Fafard, Z. Wasilewski, and P. Hawrylak, Phys. Rev. B **72**, 165353 (2005).
[5] V. Preisler, T. Grange, R. Ferreira, L. A. de Vaulchier, Y. Guldner, F. J. Teran, M. Potemski, and A. Lemaitre, Phys. Rev. B **73**, 075320 (2006).
[6] U. Bockelmann and G. Bastard, Phys. Rev. B **42**, 8947 (1990).
[7] H. Benisty, C. M. Sotomayor-Torres, and C. Weisbuch, Phys. Rev. B **44**, 10945 (1991).
[8] T. Inoshita and H. Sakaki, Phys. Rev. B **46**, 7260 (1992).
[9] U. Bockelmann and T. Egeler, Phys. Rev. B **46**, 15574 (1992).
[10] R. Strenz, U. Bockelmann, F. Hirler, G. Abstreiter, G. Böhm, and G. Weimann, Phys. Rev. Lett. **73**, 3022 (1994).
[11] D. J. Lockwood, P. Hawrylak, P. D. Wang, C. M. Sotomayor Torres, A. Pinczuk, and B. S. Dennis, Phys. Rev. Lett. **77**, 354 (1996).
[12] B. Aslan, H. C. Liu, M. Korkusinski, S.-J. Cheng, and P. Hawrylak, Appl. Phys. Lett. **82**, 630 (2003).
[13] S. Fafard and C. N. Allen, Appl. Phys. Lett. **75**, 2374 (1999).
[14] K. H. Schmidt, G. Medeiros-Ribeiro, and P. M. Petroff, Phys. Rev. B **58**, 3597 (1998).
[15] M. Grundmann, O. Stier, and D. Bimberg, Phys. Rev. B **52**, 11969 (1995).
[16] L. Chu, A. Zrenner, M. Bichler, G. Böhm, and G. Abstreiter, Appl. Phys. Lett. **77**, 3944 (2000).
[17] M. Senes, B. Urbaszek, X. Marie, T. Amand, J. Tribollet, F. Bernardot, C. Testelin, M. Chamarro, and J.-M. Gerard, Phys. Rev. B **71**, 115334 (2005).